Joint analysis of WFIRST and LSST for weak lensing

Community Astrophysics with WFIRST

Michael D. Schneider

March 2, 2016

Collaborators:
W. A. Dawson, J. Meyers, S. Schmidt, D. Bard, D. Hogg, D. Lang,
R. Mandelbaum, P. Marshall, J. Rhodes, T. Tyson

LLNL-PRES-680606
This work was performed under the auspices of the U.S. Department of Energy by Lawrence Livermore National Laboratory under contract DE-AC52-07NA27344. Lawrence Livermore National Security, LLC

Lawrence Livermore National Laboratory

Cosmic shear today & in the WFIRST era

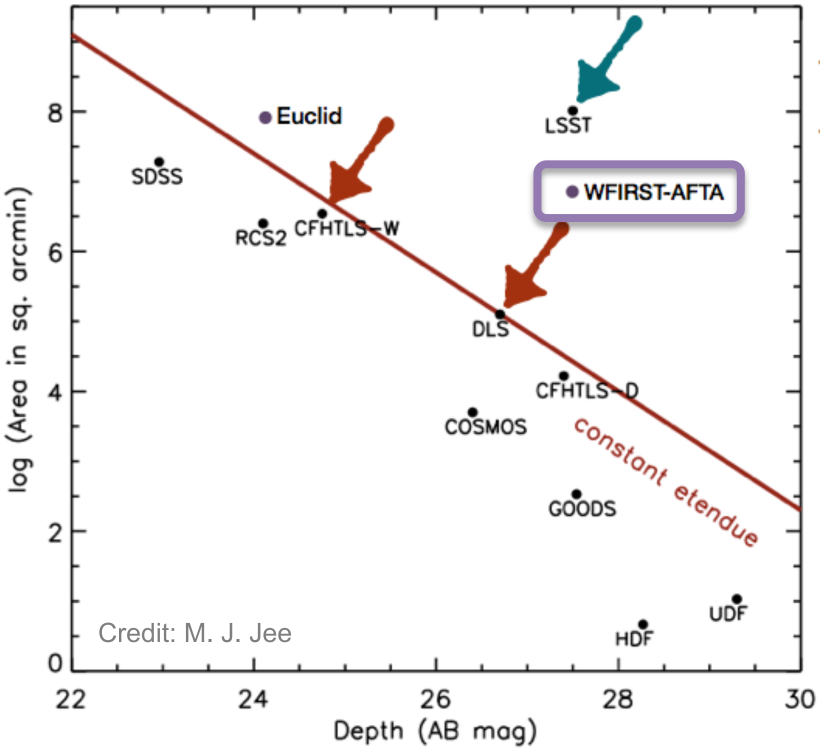

DLS shear tomography

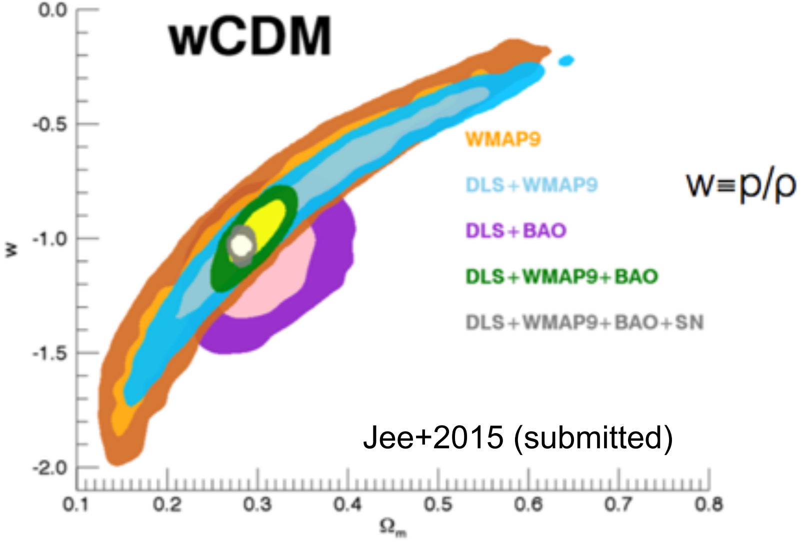

Cosmic shear is a percent-level signal
→ Need to average shapes of many galaxies

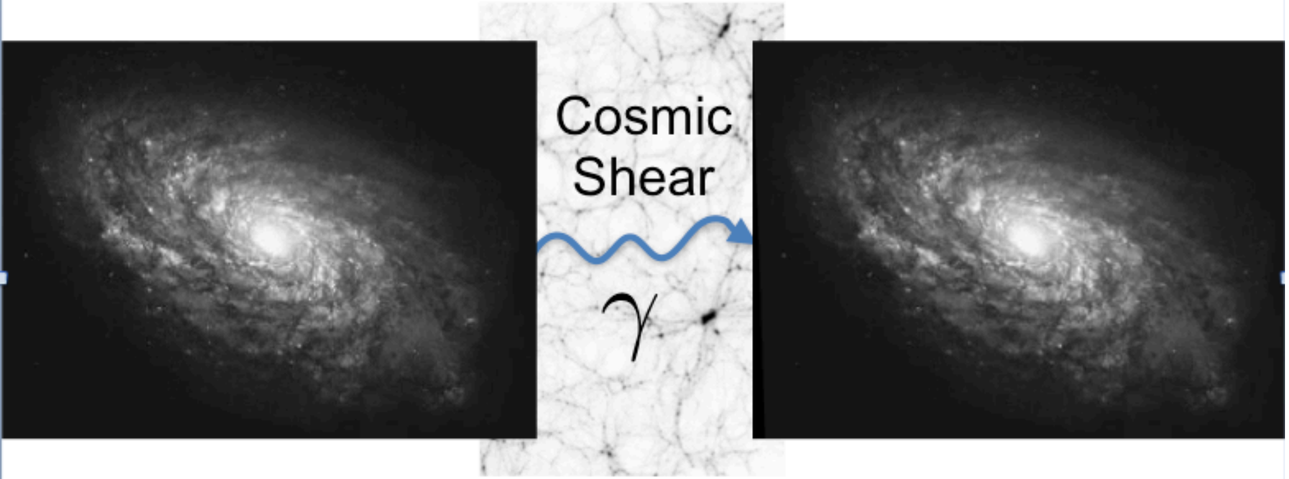

$$e_{\rm observed} \approx e_{\rm intrinsic} + \gamma$$

$$\sigma_{e_{\rm intrinsic}} \sim 0.3 \qquad \gamma \sim 0.03$$

The number density of useable galaxies for shear measurements in WFIRST-AFTA will be at least **3 times** that of LSST

Shape noise (intrinsic galaxy properties) is only part of the problem. Many systematic errors

Joint analysis helps 'self-calibrate' instrumental systematics.

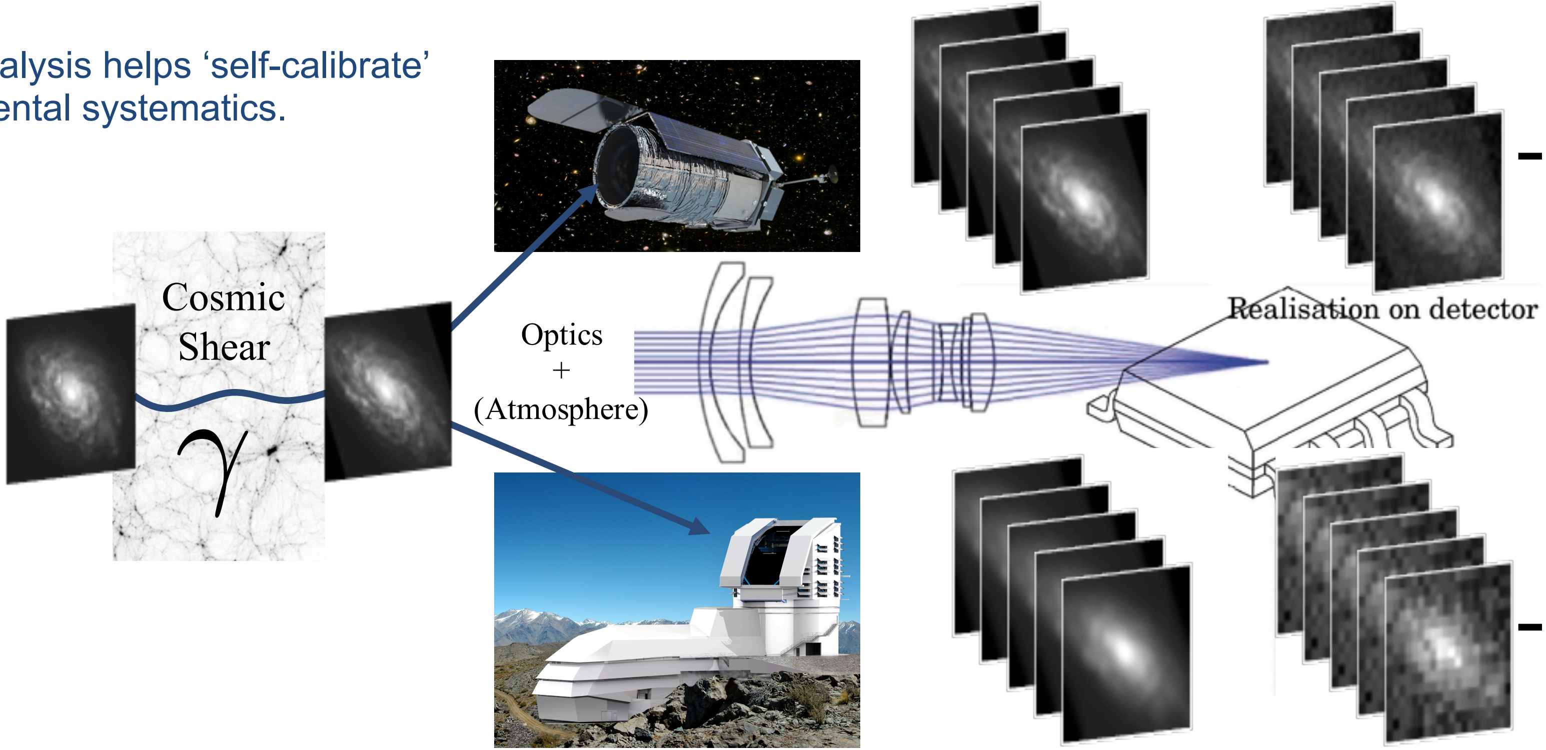

WFIRST lensing advantage: The cosmic shear signal is largest precisely where the LSST is most confused by the atmosphere

The cosmic shear correlation on sub-arcminute scales is a measure of halo substructure.

Measure of mass-to-light ratios in cross-correlation with the spectroscopic galaxy sample.

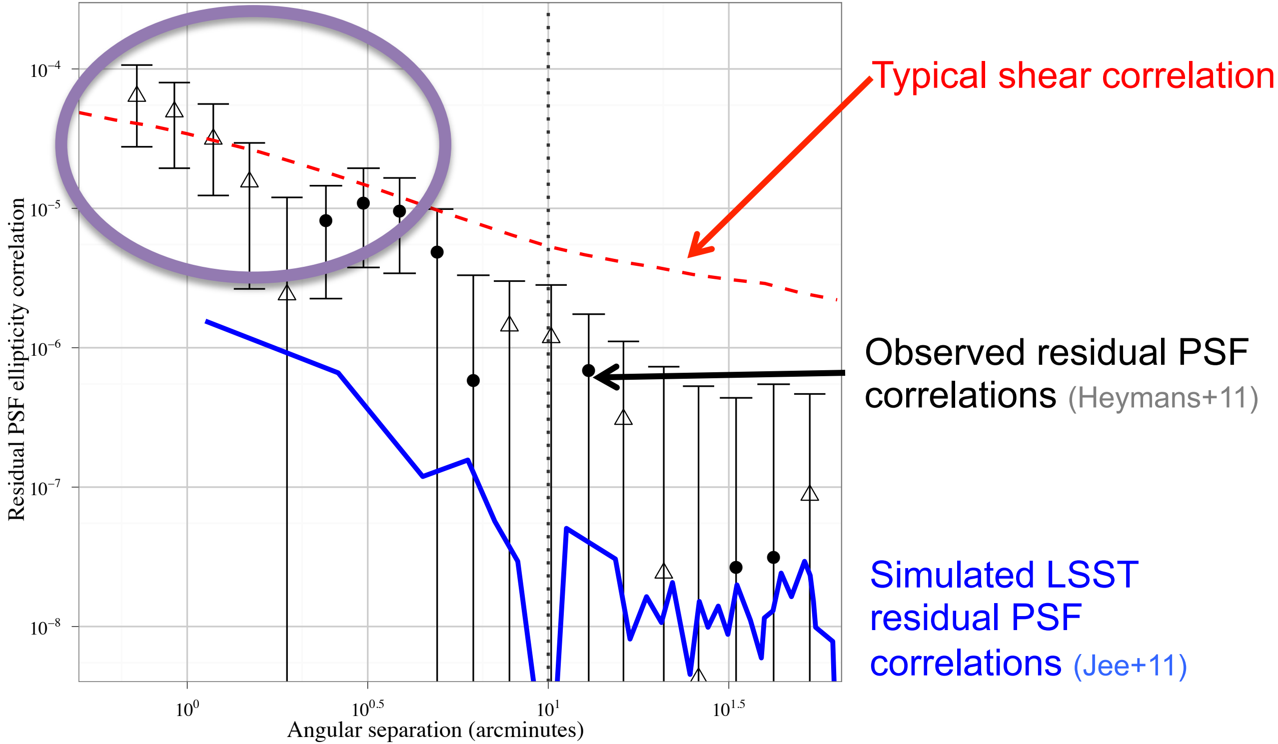

Cosmic growth constraints come from shear correlation tomography in photometric redshift bins

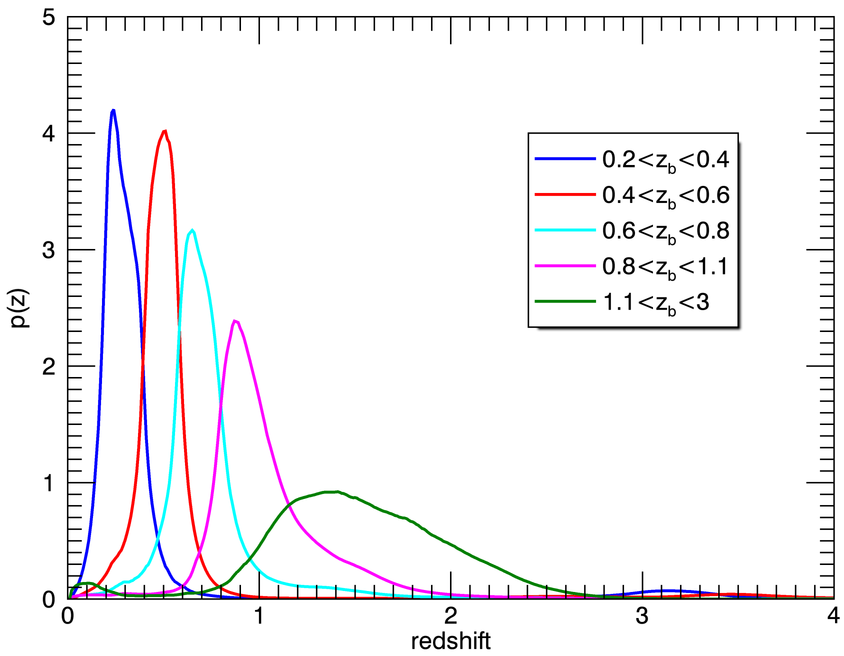

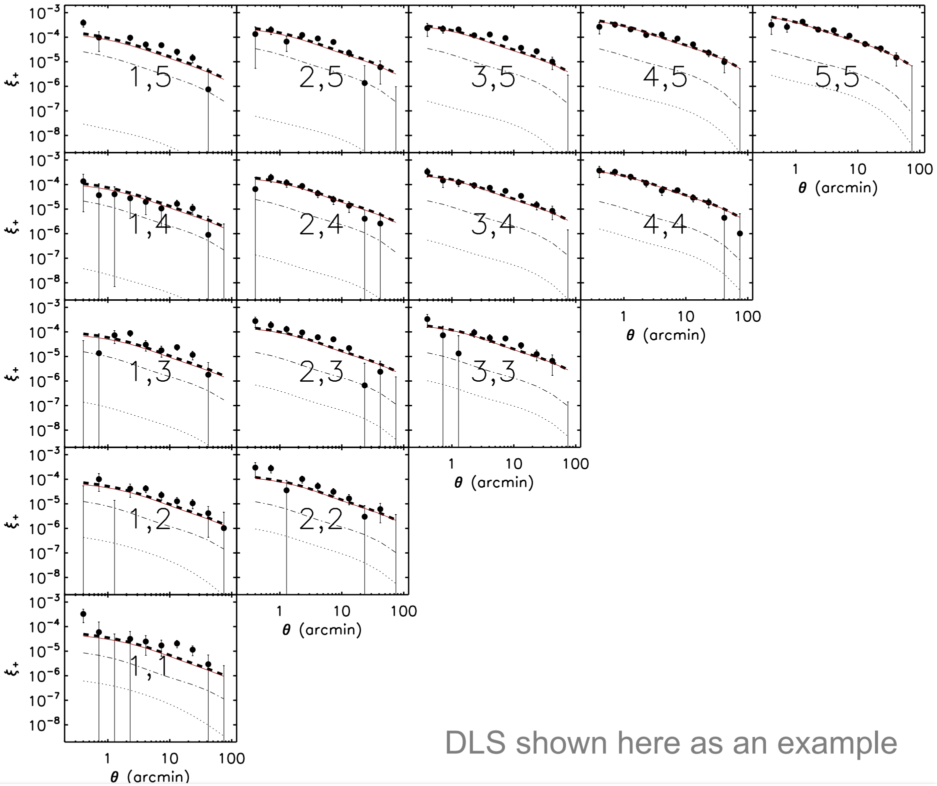

DLS shown here as an example

The 4 passbands in the High Latitude Survey do not yield useable photo-z's

- WFIRST-AFTA photo-z's limited by distinguishing features in galaxy SEDs at WFIRST wavelengths
  - not limited by photometric precision or spectroscopic training samples
- Combination with LSST 6 optical passbands is more than sufficient for shear, assuming a reliable cross-matching of catalogs can be made.

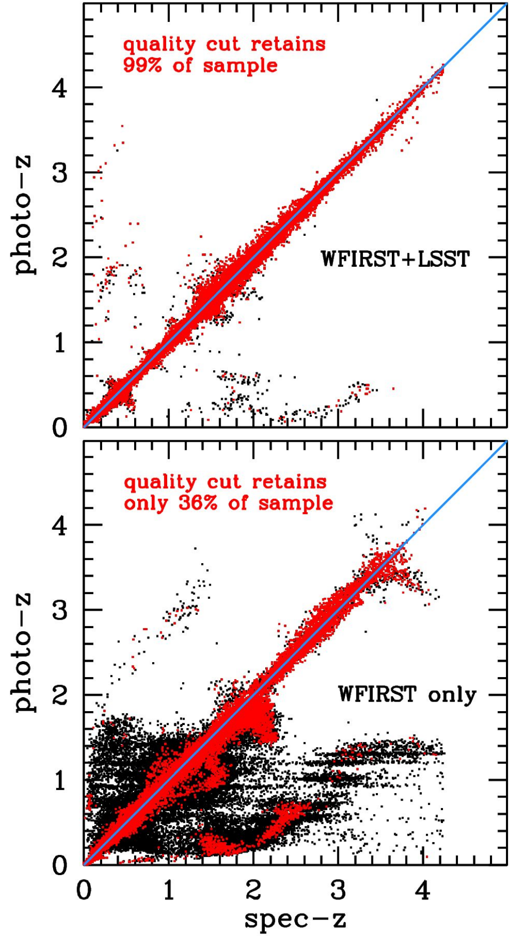

Slide: S. Schmidt

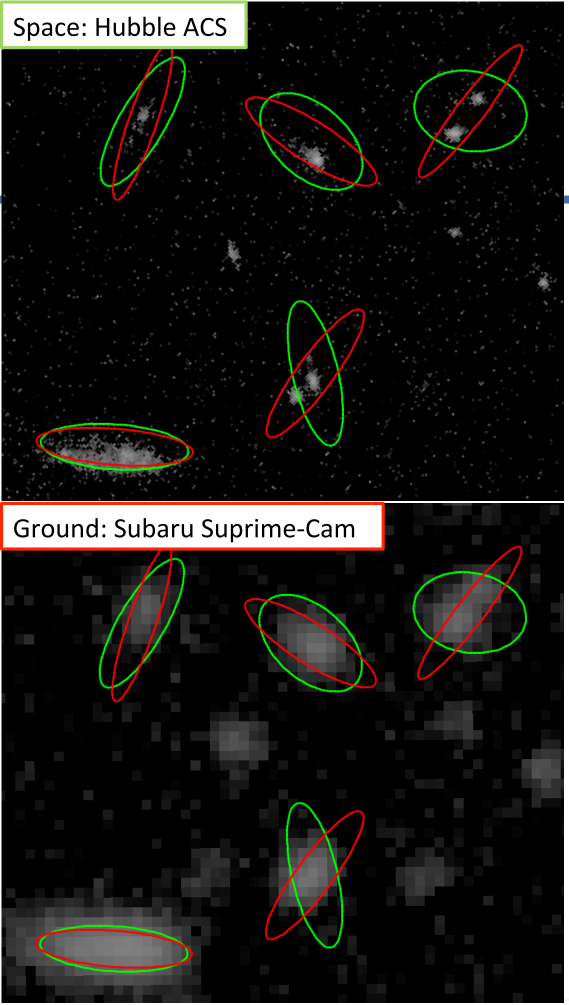

Catalog cross-matching is confused by significant object blending as seen by LSST

LSST blend fractions estimated from Subaru & HST overlapping imaging

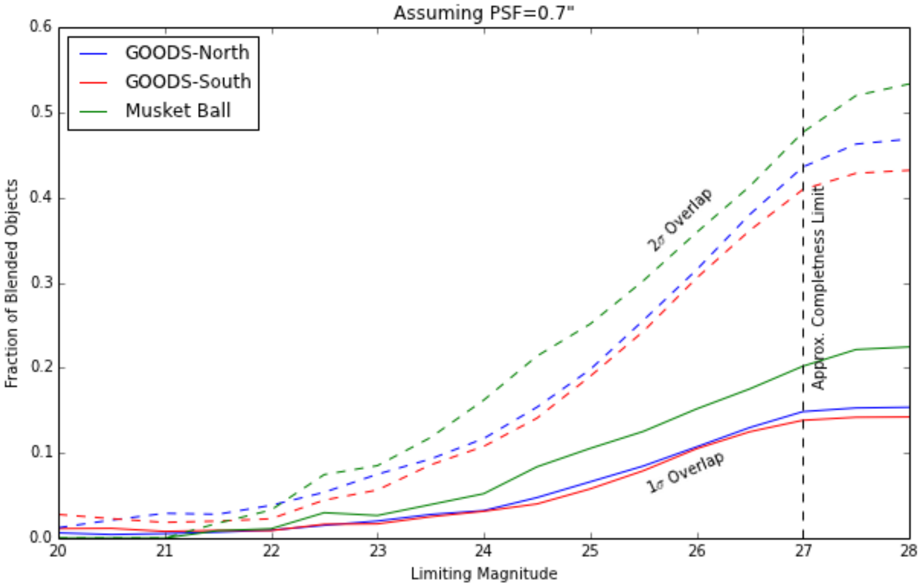

Blending and catalog cross-matching errors cause biases in the inferred redshift distribution and lensing analyses

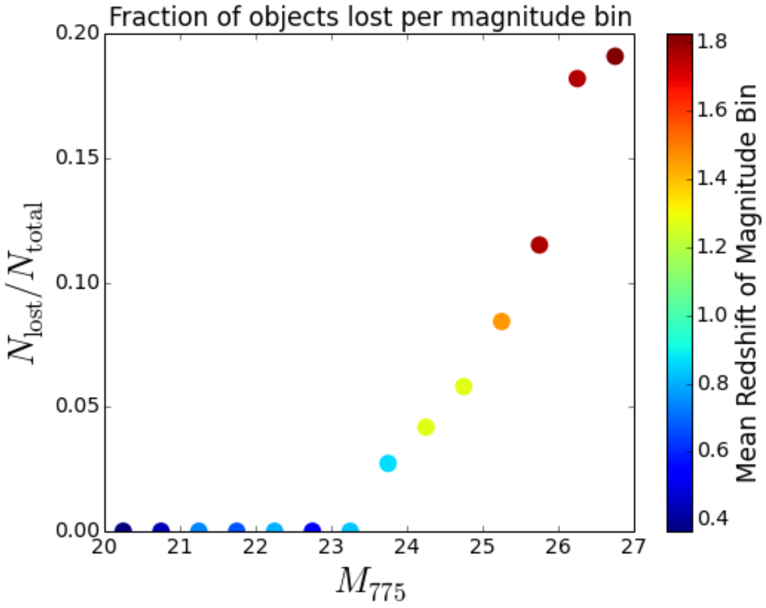

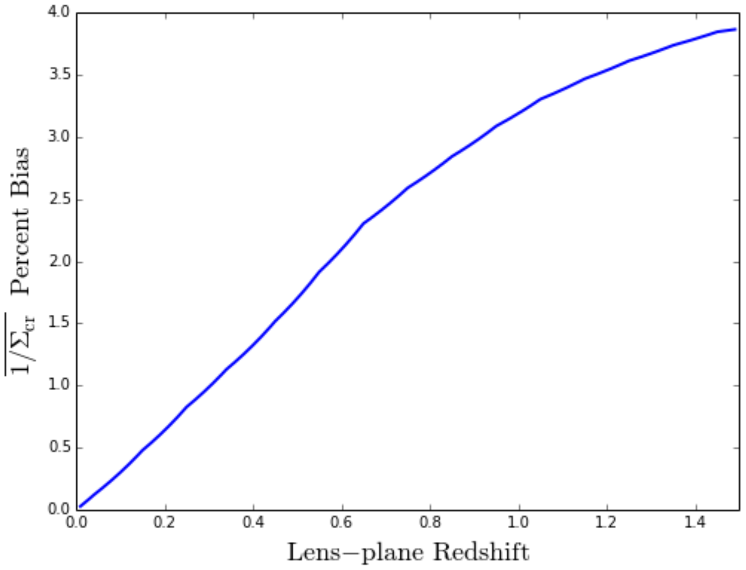

The complete statistical model for cosmic shear

arXiv:1411.2608

Parameter	Description
$\boldsymbol{\theta}$	Cosmological parameters
Ψ^{IC}	Initial conditons for the 3D gravitational potential
Ψ^{LT}	Late-time 3D gravitational potential
ψ_s	2D lens potential (given source photo-z bin s)
A_s	Parameters for the line-of-sight source distribution
$\Pi_{n_s,i}$	PSF for galaxy n_s observed in epoch i
Ω_i	Observing conditions in epoch i
$\{\omega_{n_s}\}$	Galaxy model parameters; $n_s = 1, \ldots, n_{\mathrm{gal},s}$
$\{\alpha_{n_s}\}$	Parameters for the distribution of $\{\omega_{n_s}\}$
$\{\xi_{n_s}\}$	Scaling parameters for $\{\omega_{n_s}\}$
m, τ	Hyperprior parameters for $\{\xi_{n_s}\}$
$\mathcal{A}$	Hyperparameter for $\{\alpha_{n_s}\}$ classifications
$\{\mathbf{d}_{n_s,i}\}$	Pixel data for galaxies $n_s = 1, \ldots, n_{\mathrm{gal},s}$ in epoch i
$G_0 \vert a_\eta$	Prior specification for $\{\alpha_{n_s}\}$
s	Source sample (e.g., photo-z bin)
W	Survey window function
$\mathbf{d}_{\mathrm{anc},i}$	Ancillary data for PSF in epoch i
p	Prior params. for observing conditions
a	Prior params. for $\mathcal{A}$
$\sigma_{\mathrm{pix},i}$	Pixel noise r.m.s. in epoch i
I	Model selection assumptions

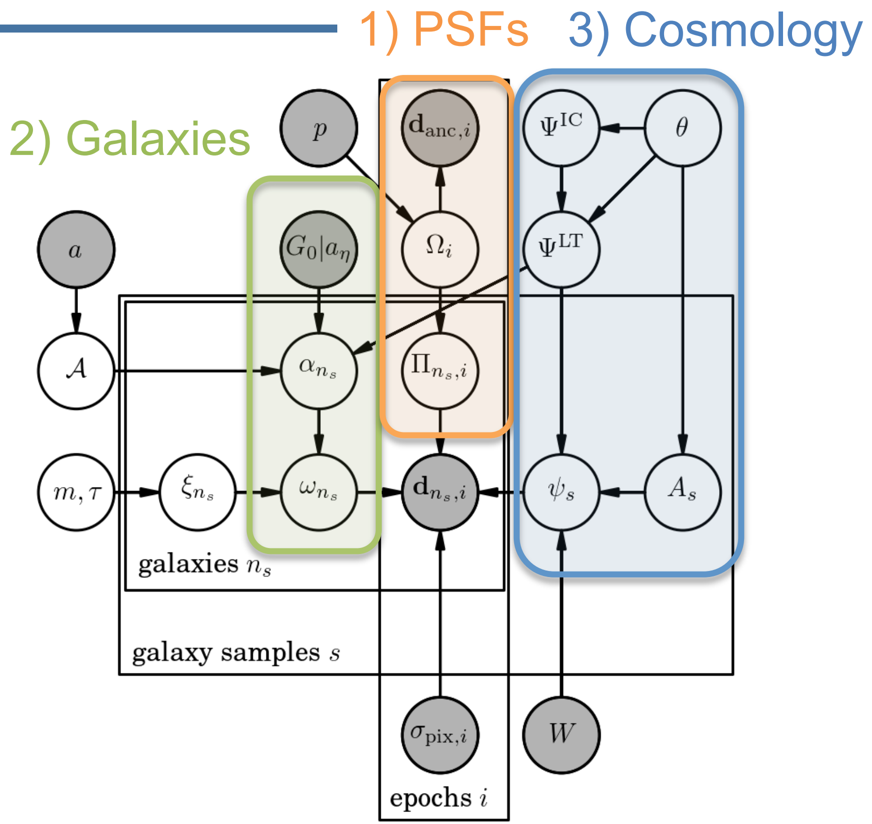

Our pipeline: 3 levels of model inference

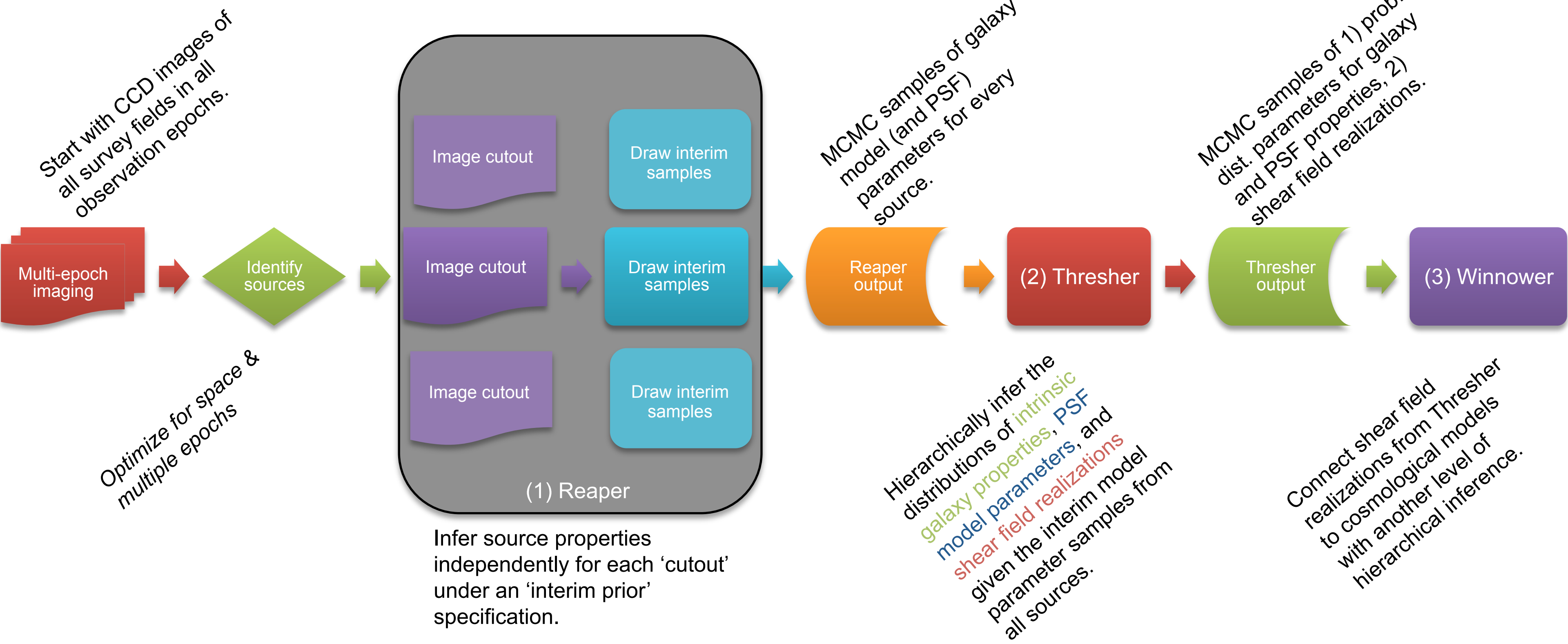

Blind, faint source detection via Maximum Likelihood significance maps

Example: HST Frontier Fields Data

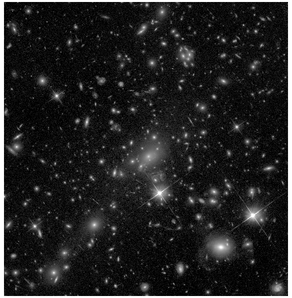

Method: J. Bosch
Slide: W. Dawson

Shallow 2 orbit image.

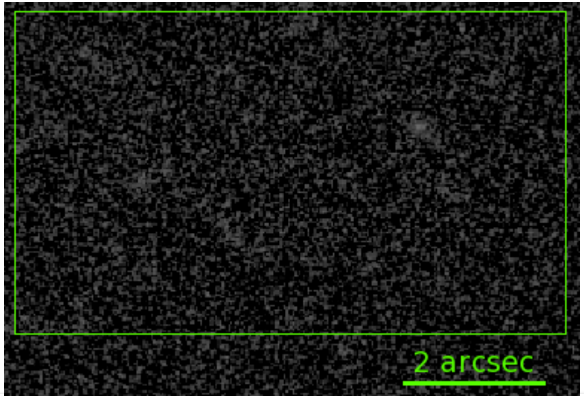

->

Detections of faint high-z lensed galaxies in faint image.

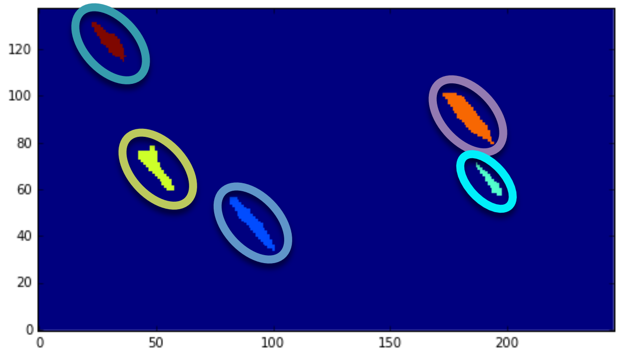

=

Deep 15 orbit image.

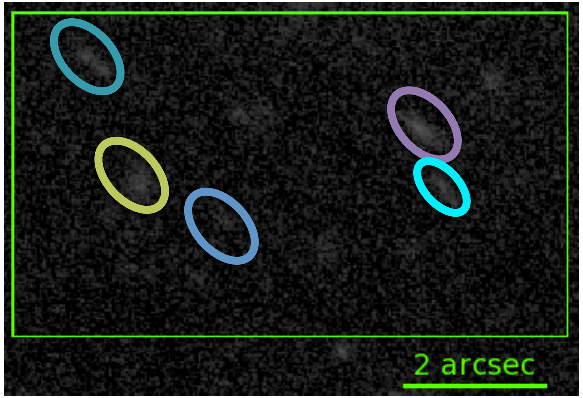

Joint Image Framework for probabilistic pixel-level source model fitting

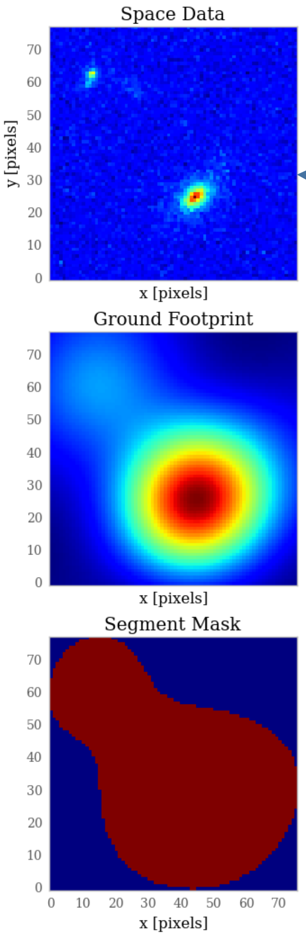

Define pixels that enter the likelihood from highest-resolution imaging.

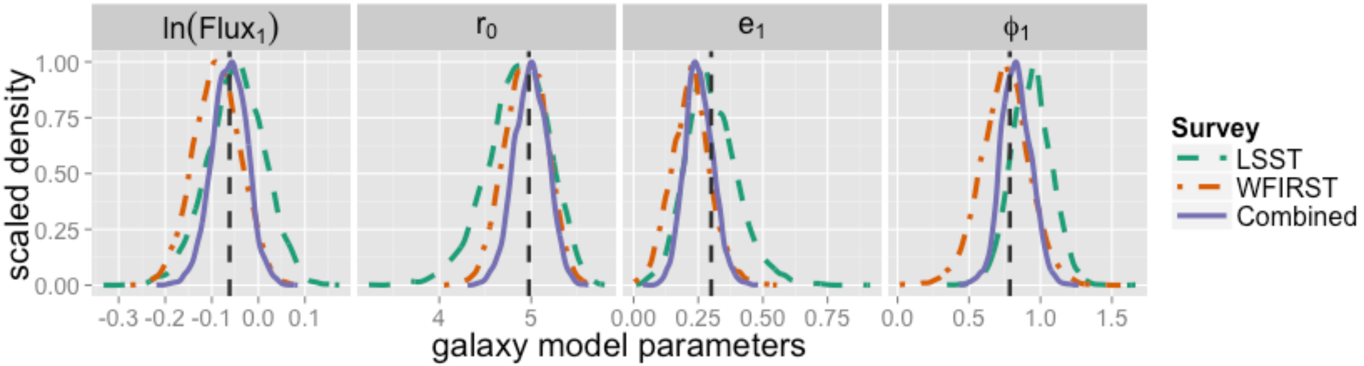

Infer joint posterior of galaxy model parameters given pixel data.

- Distinct 'footprints' connected only via hierarchical model.
- Massive parallelization with minimal information loss.

Hierarchical inference of intrinsic shape distributions reduces shear biases *without any calibration*

Test of hierarchical model with third Gravitational lEnsing Accuracy Test (GREAT3).

Hierarchical inference performs significantly better than ensemble average maximum likelihood ellipticity.

A Dirichlet Process model ellipticity priror performs better than an asserted Gaussian ellipticity prior.

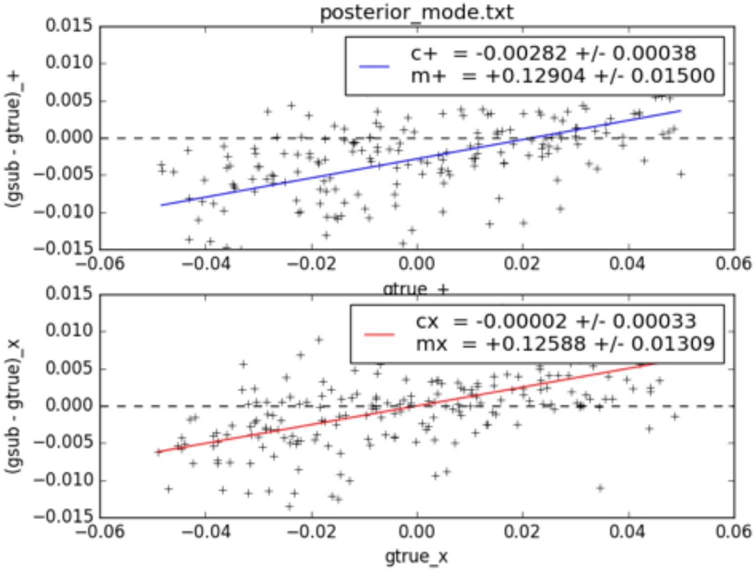

shear calibration errors

<ML>: 13%

Hierarchical inference of intrinsic shape distributions reduces shear biases *without any calibration*

Test of hierarchical model with third Gravitational lEnsing Accuracy Test (GREAT3).

Hierarchical inference performs significantly better than ensemble average maximum likelihood ellipticity.

A Dirichlet Process model ellipticity priror performs better than an asserted Gaussian ellipticity prior.

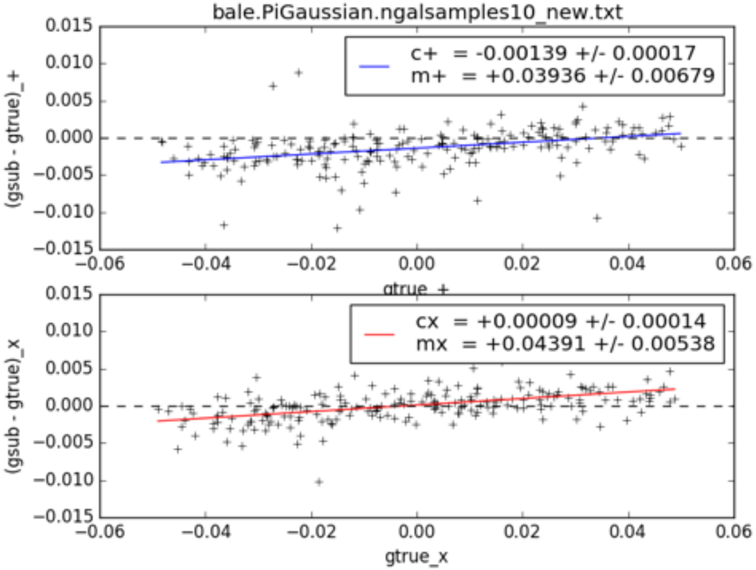

<u>shear calibration errors</u>

<ML>: 13%

H.I.: 4%

Hierarchical inference of intrinsic shape distributions reduces shear biases *without any calibration*

Test of hierarchical model with third Gravitational lEnsing Accuracy Test (GREAT3).

Hierarchical inference performs significantly better than ensemble average maximum likelihood ellipticity.

A Dirichlet Process model ellipticity priror performs better than an asserted Gaussian ellipticity prior.

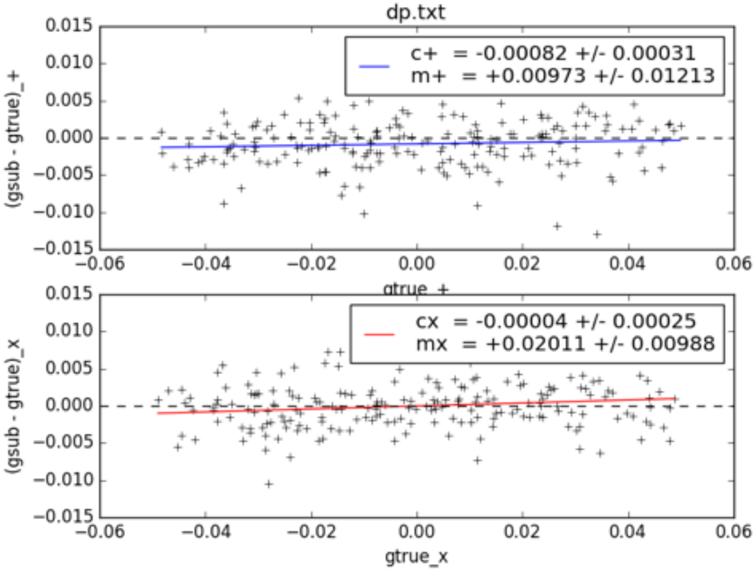

<u>shear calibration errors</u>

<ML>: 13%
H.I.: 4%
DP: 1-2%

Next - Multivariate Dirichlet Process mixture model: "standardizable" ellipticities

- Elliptical galaxies have a narrower intrinsic ellipticity distribution than late-type. Higher sensitivity to shear!

- Ellipticals / spirals also distinguishable by color and morphology (e.g., Sersic index, Gini coefficient, asymmetry), potentially providing additional variables with which to cluster.

Particular advantages for space-based imaging?

- Other correlations to exploit?

Summary

- The HLS will yield a state-of-the-art cosmic shear survey complimentary to LSST
- Joint analysis of WFIRST-AFTA and LSST imaging can reduce systematics for both surveys and lead to a better cosmic shear measurement than either survey alone.
- We are pursuing the optimal approach to joint survey analysis via pixel-level modeling and hierarchical probabilistic inference
  - Required given the ambiguous cross-matching and different detectors and PSFs
  - New science opportunities in (1) galaxy populations and (2) shear statistics

Maximum Likelihood Detection

Credit: Jim Bosch

$$m(x,\theta) = \int s(x,\theta)\phi(x)\mathrm{d}x$$ source model convolved with PSF

$$\ln\mathcal{L}\,(x,\theta) = -\tfrac{1}{2}\left[d(x) - m(x,\theta)\right]^{\mathrm{T}}\Sigma^{-1}\left[d(x) - m(x,\theta)\right] + C$$ Log likelihood

$$m(x,\theta) = \alpha\mu(x,\Theta)$$ separate the flux from the other model parameters

$$\Phi(x,\Theta) = \mu(x,\Theta)^{\mathrm{T}}\Sigma^{-1}\mu(x,\Theta)$$ noise weighted model auto-correlation

$$\Psi(x,\Theta) = d(x)^{\mathrm{T}}\Sigma^{-1}\mu(x,\Theta)$$ noise weighted data-model cross-correlation

Significance

$$\frac{\partial\ln\mathcal{L}}{\partial\alpha} = \alpha\Phi(x,\Theta) - \Psi(x,\Theta) = 0 \quad\Big|\quad \alpha_{\mathrm{ML}} = \frac{\Psi(x,\Theta)}{\Phi(x,\Theta)} \quad\Big|\quad \ln\mathcal{L}_{\mathrm{ML}} = \frac{\Psi^2(x,\Theta)}{2\Phi(x,\Theta)} \quad\Big|\quad \nu(x,\Theta) = \frac{\Psi(x,\Theta)}{\sqrt{\Phi(x,\Theta)}}$$